1. Introduction

Climate experiments with atmospheric general circulation models (AGCM) using prescribed sea surface boundary conditions are called "time-slice" experiments, and they require horizontal distribution data for sea surface temperature (SST) and sea ice concentration and thickness. Although we can use observation data sets for present-day climate experiments (AMIP-type experiments), data from atmosphere–ocean coupled general circulation models (CGCM) are often used for experiments simulating the future climate, such as that during several decades after the present or during the last decades of the 21st century. However, when we conduct a future-climate experiment by using an AGCM to evaluate possible future changes, the direct use of a CGCM's output for future boundary conditions gives rise to various problems as follows:

1. Because a CGCM's output for the present-day climate shows some bias when compared with observation data, it is difficult to evaluate future changes simply by taking the difference between AGCM results obtained by using the observed conditions and those obtained by using the output of a CGCM for future conditions.

2. By using the present-day output of a CGCM for the AGCM present-day conditions as well as for experiments on future conditions, we can evaluate future changes by taking the difference between the two results. However, it is difficult to obtain a good representation of the present-day climate with the AGCM because of the bias in the CGCM.

3. The use of the multi-model ensemble mean (MMEM) of many CGCMs for the AGCM present-day and the AGCM future conditions can cancel much of the bias of the individual models and can reduce the uncertainty in the simulated future changes, but it also cancel the interannual variability in the results of the individual models.

Therefore, it is appropriate to embed the changes from the present-day to the future in the CGCM results in the observation data and then to use those data for the AGCM simulation of future conditions, to compare with the AGCM results obtained using the observed conditions. However, the simple superposition of the changes in the observation data is problematic because the trend and interannual variability in the obtained data introduce inconsistency. This occurs especially near the ice edge, since the location of the ice edge, where future changes of sea ice are largest, differs between in the CGCM results and the observation data. As a result, the future retreat of the sea ice is not represented appropriately as described later.

In this work, we present a method for estimating the future distributions of SST and sea ice that avoids these problems by decomposing the observation data and the CGCM outputs into long-term mean, linear trend, and interannual variability, and then combining some of these components. Changes in the sea ice extent in each hemisphere are taken into account in the estimation of sea ice

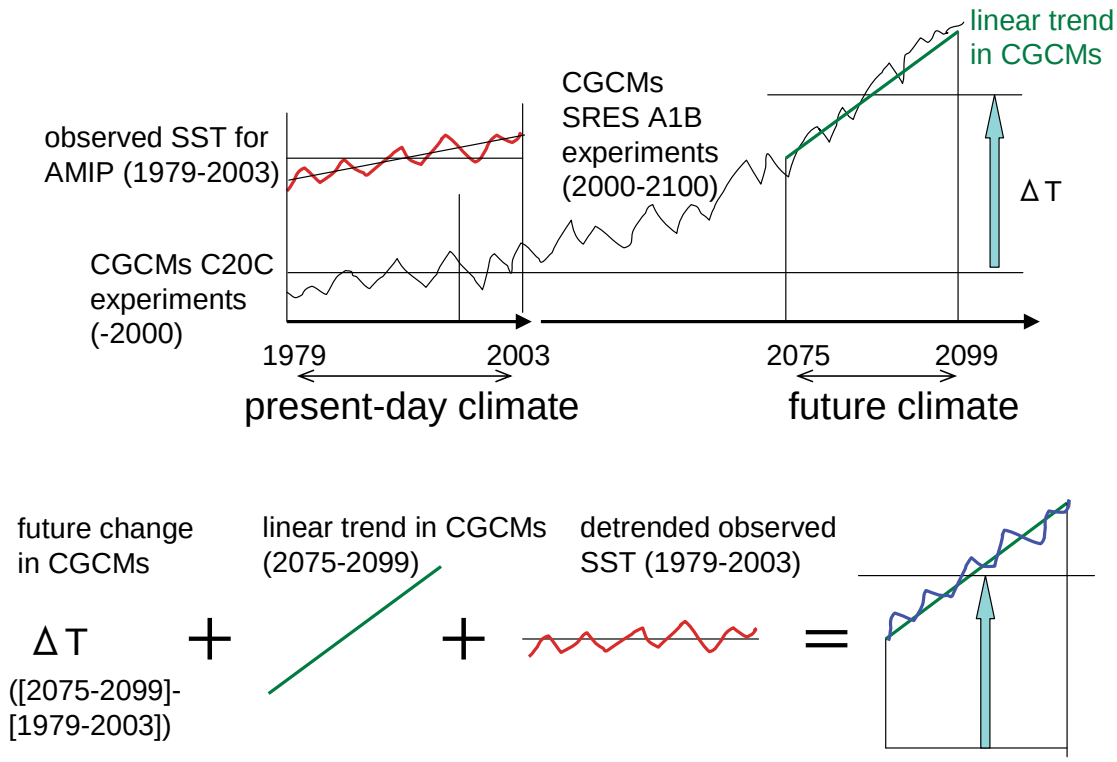

Fig. 1: The method used for estimating future SSTs.

concentrations. By using the estimated distributions of SST and sea ice for the lower boundary conditions in the AGCM experiment on future conditions and using the observed conditions for the AGCM present-day experiment, we can use the difference between the two results to represent the effect of climate change caused by the lower boundary condition changes. By also including increases in greenhouse gases and other effects in the experiments simulating future conditions, we can simulate the changes that are most likely to happen in the future.

2. Methods

2.1 Sea surface temperature

After calculating the MMEMs of the CGCMs, the MMEM and observation SSTs are decomposed into three terms as follows:

$$\begin{aligned} SST_{\mathrm{obs}}(y_1,m,x) &= SST_{\mathrm{obs\_A}}(m,x) + SST_{\mathrm{obs\_T}}(y_1,m,x) + SST_{\mathrm{obs\_V}}(y_1,m,x), \\ SST_{\mathrm{mp}}(y_1,m,x) &= SST_{\mathrm{mp\_A}}(m,x) + SST_{\mathrm{mp\_T}}(y_1,m,x) + SST_{\mathrm{mp\_V}}(y_1,m,x), \\ SST_{\mathrm{mf}}(y_2,m,x) &= SST_{\mathrm{mf\_A}}(m,x) + SST_{\mathrm{mf\_T}}(y_2,m,x) + SST_{\mathrm{mf\_V}}(y_2,m,x), \end{aligned} \qquad (1)$$

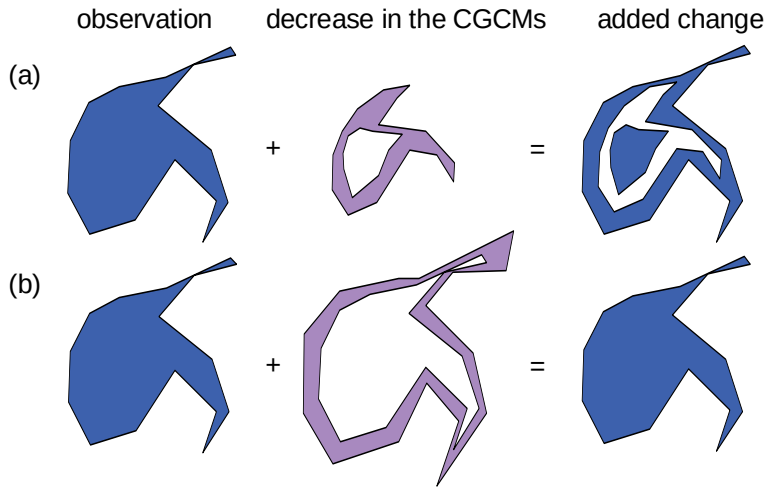

Fig. 2: Inconsistencies that can arise in the sea ice distribution when the difference between the present-day and future conditions in the CGCM results (center) is simply added to the observation data (left), when the ice edge of the CGCM is located within the observational ice edge (a), or when the MMEM ice edge is located outside the observational ice edge (b).

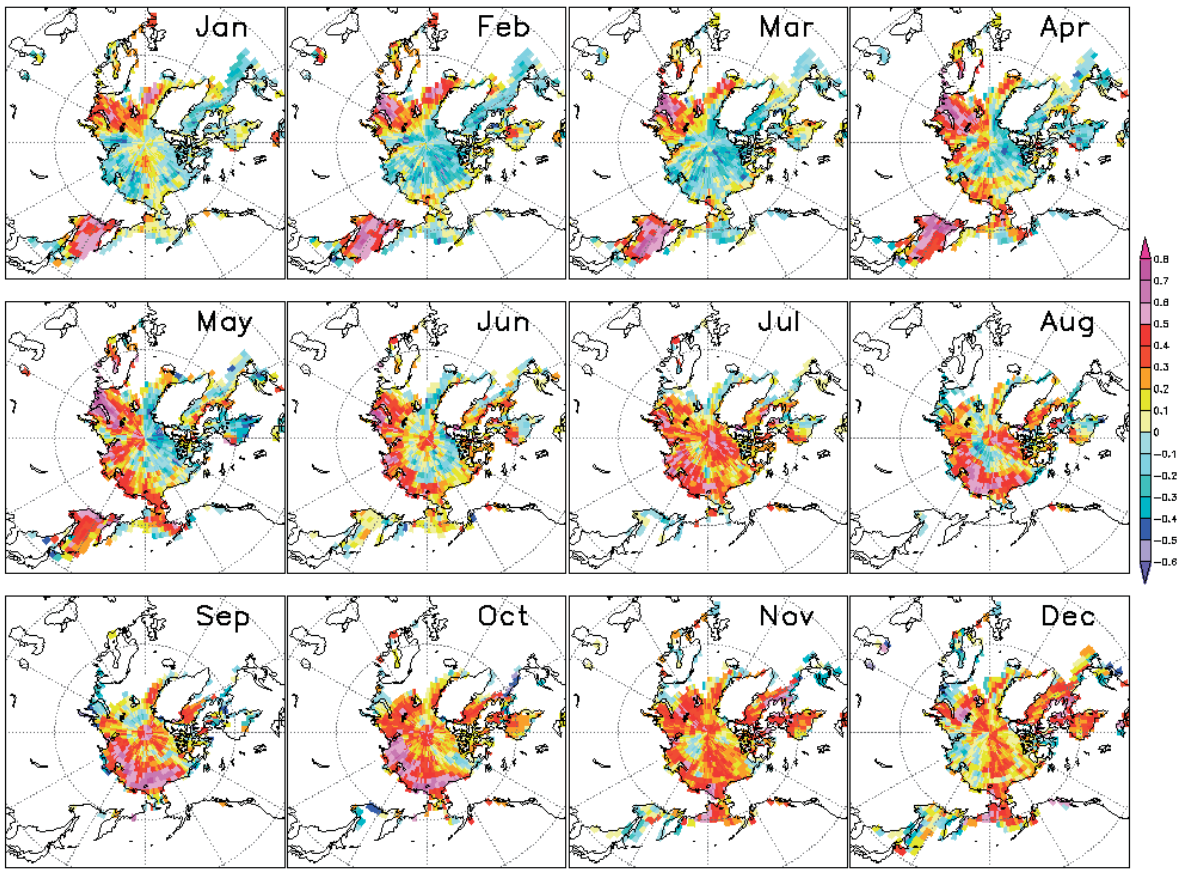

Fig. 3: Correlation coefficients between the sea ice extent in the Northern Hemisphere and the sea ice concentration at each grid point.

where obs is the observation data; mp and mf are the MMEMs for the present-day and future climate, respectively; A indicates the long-term mean; T indicates the linear trend; and V refers to the interannual variability, which is defined as the residual of A and T. Decomposition is performed at every grid point x for every month m of every year, with y_1 indicating present-day years and y_2 indicating future years.

The values of future distributions, SST_{future}, are estimated as follows:

$$SST_{\text{future}}(y_2, m, x) \equiv SST_{\text{obs\_A}}(m, x) + \left(SST_{\text{mf\_A}}(m, x) - SST_{\text{mp\_A}}(m, x)\right) + SST_{\text{mf\_T}}(y_2, m, x) + SST_{\text{obs\_V}}(y_1, m, x). \quad (2)$$

The difference between the mean present-day and future values simulated in CGCMs is a crucial component of climate change, so it is added to the observed mean to represent the estimated long-term mean. The trend in the MMEM is used as the estimated future trend. For the interannual variability, the observed variability is used as the estimated variability, under the assumption that the variability will not change in the future, because $SST_{\text{mp\_V}}$ and $SST_{\text{mf\_V}}$ are both very small owing to the cancellation of individual model variabilities. For each y_2, y_1 is chosen so that $y_2 - y_1$ is a constant value, as described in Section 3. A schematic diagram of this estimation method is presented in Figure 1.

2.2 Sea ice concentrations

If the future distribution of sea ice concentration, $fice(y_2, m, x)$, is estimated by the same method as the SST, it is highly likely that some inconsistencies will occur near the ice edge, as shown in Figure 2. This inconsistency occurs when the location of the ice edge, where the sea ice changes are largest, differs between the CGCM results and observation data. When the MMEM ice edge is located within the observational ice edge, the largest ice change also occurs within the observational ice edge. Adding the change to the observation data makes the distribution non-monotonic in the meridional direction (Fig. 2a). On the other hand, when the ice edge of the MMEM is outside the observational ice edge, little or no ice change occurs within the observational ice edge. Therefore, when the change is added to the observation data, no sea ice retreat as a result of climate change is represented (Fig. 2b).

Because the change that most affects the AGCM results is the change in the sea ice area extent, it is desirable for the change of sea ice extent between the observation data and the estimated future to be the same as the change from the CGCM present to the CGCM future. The correlations between the sea ice extent in the Northern Hemisphere and the sea ice concentration at each grid point (Fig. 3) are high, except in the center of the ice cap, where variability is small. Therefore, the sea ice concentration $fice(y_2, m, x)$ in the future can be estimated from the change in the sea ice extent in each hemisphere as follows (Fig. 4):

1. In each hemisphere, the sea ice extent, *Sice*, is defined as a function of the sea ice concentration *f*,

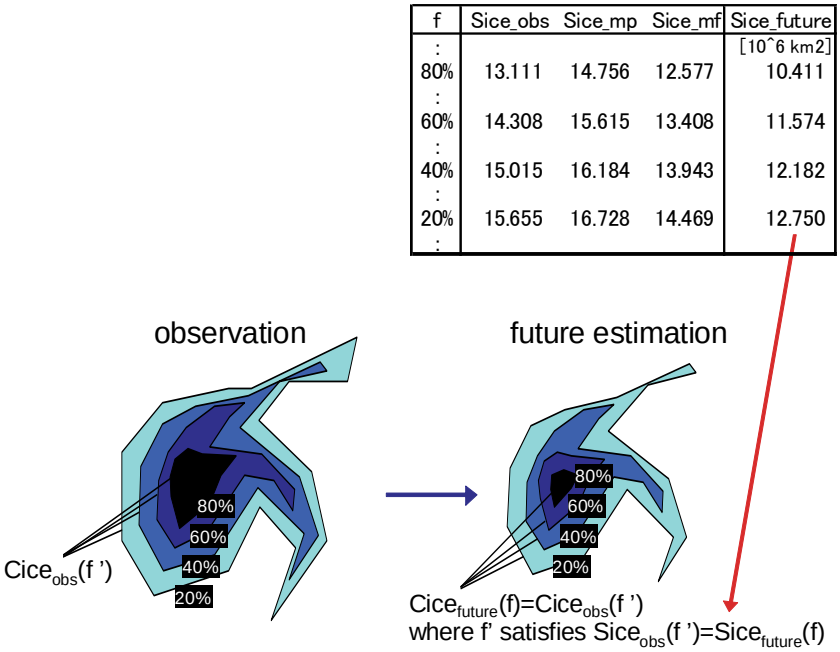

Fig. 4: Diagram of the method used for estimating future sea ice concentrations. $Sice_{obs}$, $Sice_{mp}$, and $Sice_{mf}$ are functions of f. The example values in the table (top) are for y_1 = 1994, y_2 = 2090, and m = 3 in the Northern Hemisphere. (bottom) The correspondence between $Cice_{obs}$ (y_1, m, h, f), and $Cice_{future}$ (y_2, m, h, f).

so that $Sice(f)$ is the area in which the concentration is more than f. The extent in every month m of every year y is calculated separately for each hemisphere h.

2. The sea ice extent in the future is estimated in the same way as SST (Eq. 2) by using the monthly sea ice extent, $Sice$:

$$Sice_{future}(y_2, m, h, f) \equiv Sice_{obs\_A}(m, h, f) + \left(Sice_{mf\_A}(m, h, f) - Sice_{mp\_A}(m, h, f)\right) + Sice_{mf\_T}(y_2, m, h, f) + Sice_{obs\_V}(y_1, m, h, f). \quad (3)$$

3. For each month, $fice_{future}(y_2, m, x)$ in the future is estimated by shrinking the observed extent, $fice_{obs}(y_1, m, x)$, while keeping the shape of the ice cap, until $Sice_{future}(y_2, m, h, f)$ is equal to Eq. (3). To do so, we prepare the isopleth shapes $Cice_{obs}(y_1, m, h, f)$ as a function of f for the observed sea ice distribution (Fig. 4, left), obtaining the correspondence between f, $Sice_{obs}$ (y_1, m, h, f), and $Cice_{obs}$ (y_1, m, h, f). Next, we find f' for each f that satisfies

$$Sice_{obs}(y_1, m, h, f') = Sice_{future}(y_2, m, h, f). \quad (4)$$

Then, the isopleth f in the future is estimated by

$$Cice_{future}(y_2, m, h, f) \equiv Cice_{obs}(y_1, m, h, f'). \quad (5)$$

By combining $Cice_{future}$ (y_2, m, h, f) estimated for f from 0% to 100%, we can obtain the estimated distribution of sea ice concentrations in the future.

2.3 Sea ice thickness

The sea ice thickness in the future is estimated so that the rate of change in the sea ice volume is equal to the rate of change in the MMEM results. For simplicity, the estimated thickness distribution $dice_{future}(m, x)$ defined for each month is obtained by multiplying the observed thickness distribution by a constant α:

$$dice_{future}(m,x) \equiv \alpha \cdot dice_{obs}(m,x). \qquad (6)$$

Here, since we have only the climatology of the thickness observations and do not have reliable observed trends or interannual variability, we use a future thickness distribution that has only seasonal variation and no interannual variability.

The constant α is obtained as follows (Fig. 5). First, the sea ice volume, *Vice*, in each hemisphere for the observation data and the MMEM is calculated:

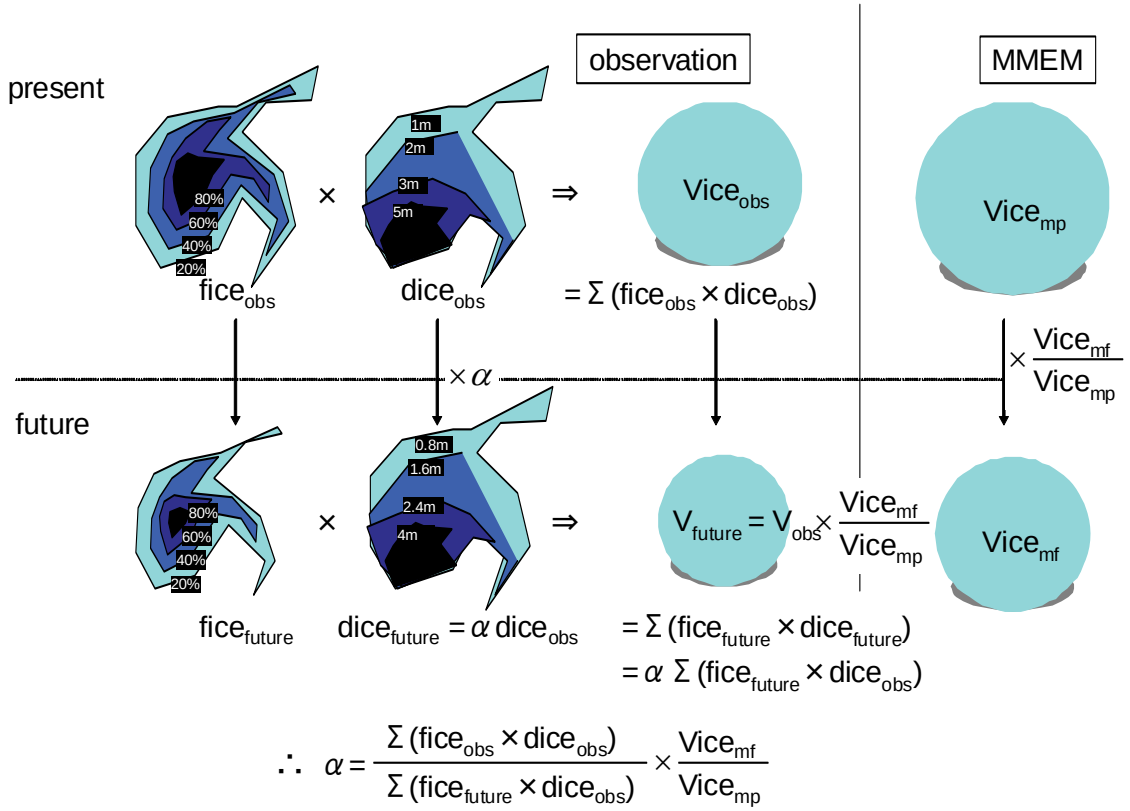

Fig. 5: Diagram of the method used for estimating future sea ice thickness.

$$
\begin{aligned}
Vice_{\mathrm{obs}}(m,h) &= \sum_{x,y1}\left\{fice_{\mathrm{obs}}(y_1,m,x)\times dice_{\mathrm{obs}}(m,x)\right\},\\
Vice_{\mathrm{mp}}(m,h) &= \sum_{x,y1}\left\{fice_{\mathrm{mp}}(y_1,m,x)\times dice_{\mathrm{mp}}(y_1,m,x)\right\},\\
Vice_{\mathrm{mf}}(m,h) &= \sum_{x,y2}\left\{fice_{\mathrm{mf}}(y_2,m,x)\times dice_{\mathrm{mf}}(y_2,m,x)\right\}.
\end{aligned}
\tag{7}
$$

Sea ice volume $Vice_{\mathrm{future}}(m, h)$ in the future is estimated so that the rate of change from the observation data is equal to the rate of change in the MMEM results:

$$
Vice_{\mathrm{future}}(m,h) \equiv Vice_{\mathrm{obs}}(m,h)\times\frac{Vice_{\mathrm{mf}}(m,h)}{Vice_{\mathrm{mp}}(m,h)}. \tag{8}
$$

Since

$$
\begin{aligned}
Vice_{\mathrm{future}}(m,h) &= \sum_{x,y2}\left\{fice_{\mathrm{future}}(y_2,m,x)\times dice_{\mathrm{future}}(m,x)\right\}\\
&= \sum_{x,y2}\left\{fice_{\mathrm{future}}(y_2,m,x)\times \alpha dice_{\mathrm{obs}}(m,x)\right\}\\
&= \alpha\sum_{x,y2}\left\{fice_{\mathrm{future}}(y_2,m,x)\times dice_{\mathrm{obs}}(m,x)\right\},
\end{aligned}
\tag{9}
$$

α can be calculated by

$$
\alpha = \frac{\sum_{x,y1}\left\{fice_{\mathrm{obs}}(y_1,m,x)\times dice_{\mathrm{obs}}(m,x)\right\}}{\sum_{x,y2}\left\{fice_{\mathrm{future}}(y_2,m,x)\times dice_{\mathrm{obs}}(m,x)\right\}}\times\frac{Vice_{\mathrm{mf}}(m,h)}{Vice_{\mathrm{mp}}(m,h)}. \tag{10}
$$

Table 1: Data sets used for the CMIP3 models.

Name	Institute
bccr_bcm2_0	Bjerknes Centre for Climate Research, Norway
cccma_cgcm3_1	Canadian Centre for Climate Modeling & Analysis, Canada
cccma_cgcm3_1_t63	
cnrm_cm3	Météo-France/Centre National de Recherches Météorologiques, France
csiro_mk3_0	CSIRO Atmospheric Research, Australia
gfdl_cm2_0	U.S. Dept. of Commerce/NOAA/Geophysical Fluid Dynamics Laboratory, USA
gfdl_cm2_1	
giss_aom	NASA/Goddard Institute for Space Studies, USA
inmcm3_0	Institute for Numerical Mathematics, Russia
ipsl_cm4	Institut Pierre Simon Laplace, France
miroc3_2_hires	Center for Climate System Research (University of Tokyo), National Institute for Environmental Studies, and Frontier Research Center for Global Change (JAMSTEC), Japan
miroc3_2_medres	
miub_echo_g	Meteorological Institute of the University of Bonn, Meteorological Research Institute of KMA, and Model & Data Group, Germany/Korea
mpi_echam5	Max Planck Institute for Meteorology, Germany
mri_cgcm2_3_2a	Meteorological Research Institute, Japan
ncar_ccsm3_0	National Center for Atmospheric Research, USA
ukmo_hadcm3	Hadley Centre for Climate Prediction and Research/Met Office, UK
ukmo_hadgem1	

3. Verification of the estimated distributions

We estimated the distributions for 2015–2039 and 2075–2099 by this method using the observation data and the MMEM. Monthly mean data from the Hadley Center (Rayner et al., 2003) from 1979 to 2003 were used for the observed SST and sea ice concentration data, along with the monthly climatology of sea ice thickness from Bourke and Garrett (1987). The results of the Climate of the Twentieth Century Project (C20C) experiments (until 2000) and the SRES A1B scenario experiments (after 2000) of 18 CMIP3 CGCMs (Meehl et al. 2007) were used for the MMEM. The CGCMs used here are listed in Table 1. We used only one experiment from models with multiple experiments. Phases of the observed interannual variability SST_{obs_V} during y_1 = 1979, … , 2003 were shifted 36 or

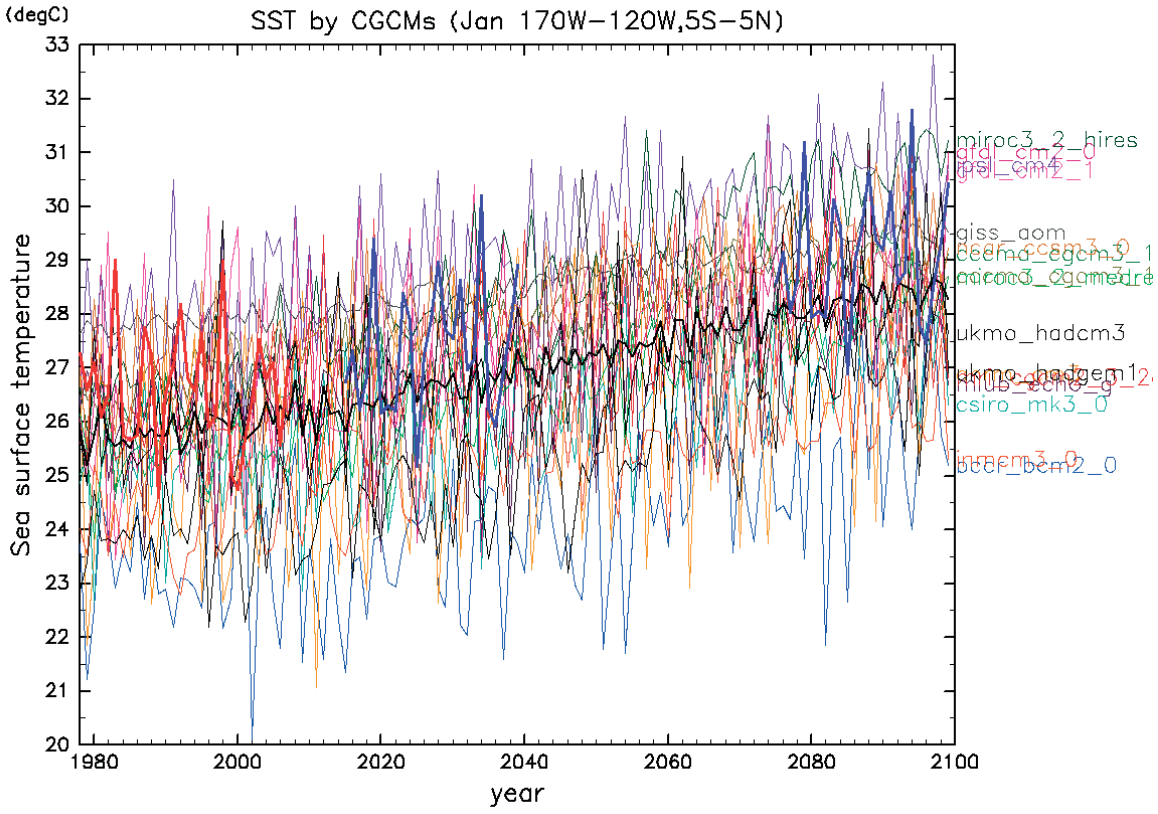

Fig. 6: Sea surface temperatures averaged over 170°W–120°W and 5°S–5°N in January. Thin lines are the CGCM results, and the thick black line is the ensemble mean of the CGCM results. The thick red line is the observation data, and the thick blue lines denote SST_{future}, estimated by Eq. (2) for 2015–2039 and 2075–2099.

96 years to y_2 = 2015, … , 2039 or y_2 = 2075, … , 2099 for use in Eqs. (2) and (3). For example, y_1 = 1979 was used with y_2 = 2015 or y_2 = 2075, and y_1 = 1980 was used with y_2 = 2016 or y_2 = 2076. This same correspondence between y_1 and y_2 was also used when shrinking the sea ice distribution (Eqs. (4) and (5)). In Eq. (5), we calculated $Cice_{\text{future}}$ (y_2, m, h, f) for f with intervals of 0.1%.

Figure 6 shows SST averaged over the tropical Pacific region in the observation data, the CGCMs, the MMEM, and the estimated future. The variability in this region is mainly due to ENSO. Although each CGCM (thin colored lines) shows more or less interannual variability, the MMEM (thick black line) shows very small variability because of cancellation of variation phases. Since the observed SST (thick red line) is higher than the MMEM by about 0.7 K, the estimated SST (thick blue lines) obtained by Eq. (2) is also higher than the MMEM.

Figure 7 shows Northern Hemisphere sea ice concentrations in March during three observation years (y_1 = 1994, 1998, and 2002), and estimated concentrations in three future years (y_2 = 2090, 2094, and 2098). In the future estimations, sea ice decreases and retreats around Newfoundland and the Sea of

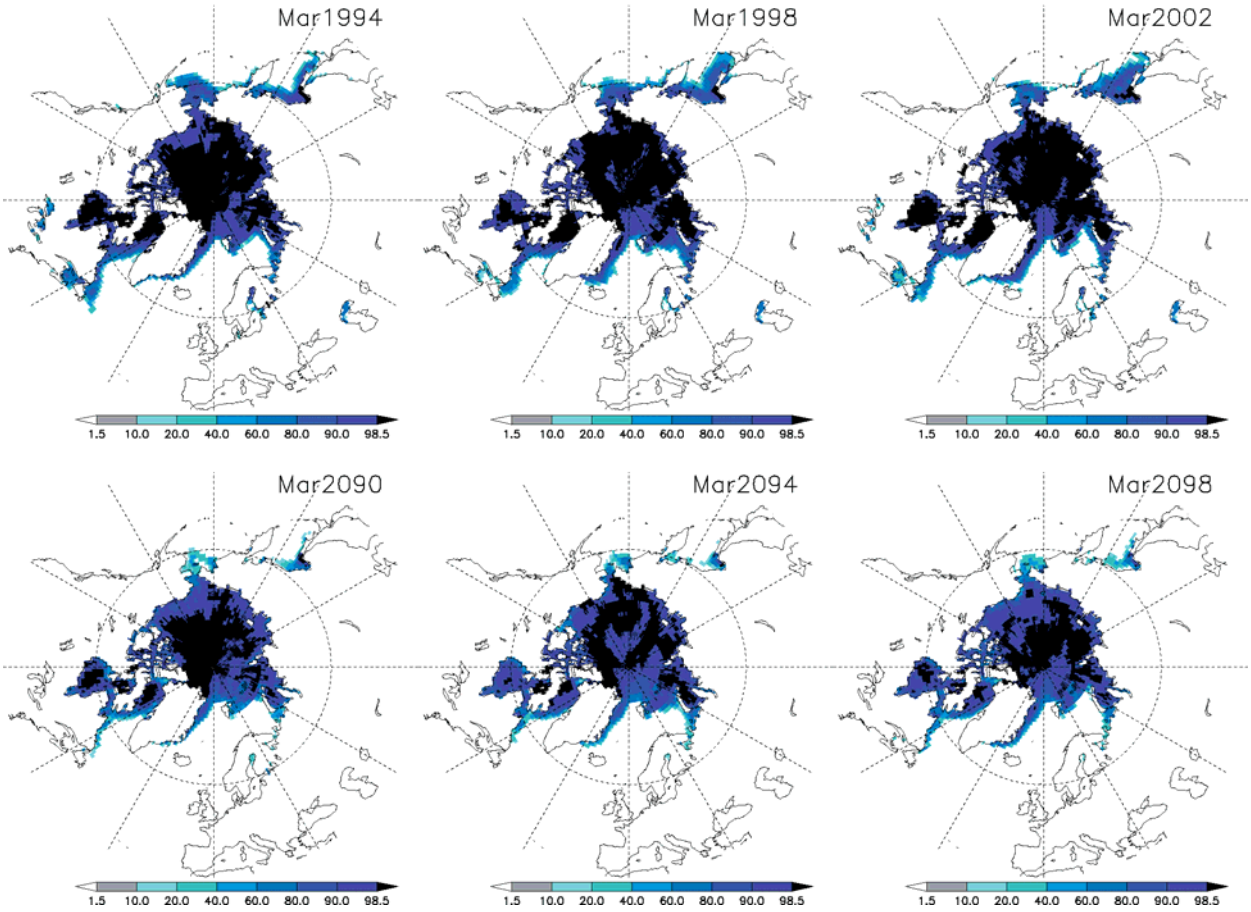

Fig. 7: Horizontal distributions of sea ice concentrations in March in the observation data, $fice_{\mathrm{obs}}(y_1, m, x)$ (top), and estimated $fice_{\mathrm{future}}(y_2, m, x)$ in the future (bottom).

Okhotsk. Some interannual variability in the observation data is apparent: in 1994, more sea ice was observed in the Western Hemisphere, and in 1998, more was observed in the Eastern Hemisphere. This kind of variability is kept in the estimated distribution: There is more sea ice in the Western Hemisphere in 2090 and more in the Eastern Hemisphere in 2094, because in Eq. (5) the sea ice distribution in y_2 is calculated using the isopleths of the sea ice concentration in y_1.

As supplemental information, monthly SST, sea ice concentration, and sea ice thickness and their changes averaged over the 25 years, along with monthly $SST_{\mathrm{mf\_T}}$ and $SST_{\mathrm{obs\_V}}$, are shown in Figs. S1–S16.

4. Discussion

There is large uncertainty with regard to the future changes in the amplitude and horizontal pattern of interannual variability. A variety of changes in ENSO are found in CMIP3 CGCMs (IPCC 2007). Whereas a linear trend induced by the greenhouse gas increase is dominant in the linear trend of the

MMEM future experiments, that is not the case in the present-day climate (either in the observation data or the MMEM present experiments). Decadal variability accounts for the calculated linear trend in the present-day climate to a certain degree, mainly because of the short time period of the data. In this work, therefore, we used observation data alone for estimating future interannual variability, and MMEM future results alone for estimating the future linear trend. Correction of the bias in the linear trend between the MMEM present and the observation data might be desirable if the effect of decadal variability could be removed from the calculated linear trend.

If we take the median sea ice concentration of the present-day CGCM experiments, a distribution very similar to the observation data is obtained. Thus, it would be possible to estimate the long-term mean of the locations of future decreases by calculating $fice_{mf} - fice_{\mathrm{mp}}$. However, interannual variability in the location of the decrease is not represented in such a calculation because interannual variability in MMEM is very small as a result of cancellations.

The estimated SST, sea ice concentration, and sea ice thickness have been used as boundary conditions in simulations of an AGCM with a horizontal grid size of 20 km performed by the Earth Simulator. Although the method described in this work would have difficulty estimating values for the very near future, when the phases of the interannual variation would be continuous with the present-day observation data, it is nevertheless one of the most objective methods available by which to estimate sea surface conditions 10 to 100 years from now by using the MMEM results.

Supplementary Information

Monthly SST, sea ice concentration, and sea ice thickness, their changes averaged over the 25 years, and monthly $SST_{\mathrm{mf\_T}}$ and $SST_{\mathrm{obs\_V}}$, are shown in Supplemental Figs. S1–S16.

Acknowledgements

This work was supported by the "Projection of Change in Future Weather Extremes Using Super-High-Resolution Atmospheric Models" project as a part of the KAKUSHIN Program of the Ministry of Education, Culture, Sports, Science and Technology of Japan, and by the Global Environment Research Fund (S-5-2) of the Ministry of the Environment of Japan.

References

Bourke, R.H. and R.P. Garrett, 1987: Sea ice thickness distribution in the Arctic Ocean. *Cold Regions Sci. and Tech.*, **13**, 259-280.

Intergovernmental Panel on Climate Change, 2007: Climate change 2007: The Physical Science Basis—Contribution of the Working Group I to the Fourth Assessment Report of the